Eur. Phys. J. Plus (2018) **133**: 289
DOI 10.1140/epjp/i2018-12133-8

THE EUROPEAN PHYSICAL JOURNAL PLUS

Regular Article

Dispersive optical soliton solutions of the higher-order nonlinear Schrödinger dynamical equation via two different methods and its applications

E. Tala-Tebue[1,2], Aly R. Seadawy[3,4,a], P.H. Kamdoum-Tamo[2,5], and Dianchen Lu[6]

[1] Laboratoire d'Automatique et d'Informatique Appliquée (LAIA), IUT-FV of Bandjoun, The University of Dschang, BP 134, Bandjoun, Cameroon
[2] Laboratory of Mechanics, Department of Physics, Faculty of Sciences, and African Center of Excellence in I.C.T (C.E.T.I.C) University of Yaounde I, P.O. Box 812, Yaoundé, Cameroon
[3] Mathematics Department, Faculty of Science, Taibah University, Al-Madinah Al-Munawarah, Saudi Arabia
[4] Mathematics Department, Faculty of Science, Beni-Suef University, Beni-Suef, Egypt
[5] Nonlinear Physics and Complex Systems Group, Department of Physics, The Higher Teachers' Training College, University of Yaounde I, P.O. Box 47 Yaoundé, Cameroon
[6] Department of Mathematics, Faculty of Science, Jiangsu University, Zhenjian, China

Received: 5 May 2018 / Revised: 11 June 2018
Published online: 31 July 2018

Abstract. In this paper, we apply two methods which are the arbitrary nonlinear parameters and the exponential rational function method to construct many new exact solutions of the higher-order nonlinear partial differential equations, namely, the higher-order nonlinear Schrödinger (HNLS) equation. The solutions obtained by the current methods are generalized periodic solutions. The shape of the solutions can be well controlled by adjusting the parameters of the system. Optical soliton solutions obtained can be used to transport information in the telecommunication domain. It also comes from this work that the behavior of this HNLS equation may be easily studied by means of the phase plane plot which is the best tool to predict some solutions.

1 Introduction

Since the first observation of a soliton by John Scott Russell in 1834 [1], this type of solitary wave with exceptional stability has fascinated scientists; primarily because of their spectacular experimental properties and their undeniable elegances, but also due to their mathematical properties. Soliton research has been conducted in diverse fields such as meteorology, nonlinear electrical lines, biology, cosmology and optical fibers, to cite a few. Optical solitons have promising potential to become principal information carriers in telecommunication due to their capability of propagating a long distance without attenuation and changing their shapes. The pioneering works of Hasegawa and Tappert [2], who predicted solitons theoretically, and Mollenauer, Stolen, and Gordon [3], who observed them experimentally, made solitons a realistic tool for this cause. In a single mode fiber, the pulse envelope function satisfies a nonlinear Schrödinger (NLS) equation [4] in the following form:

$$iE_z - \alpha_1 E_{tt} - \alpha_2 |E|^2 E = 0, \tag{1}$$

where z is the propagation direction of the pulse, t is the retarded-time variable, $E = E(z,t)$ is the pulse envelope function, α_1 and α_2 are constants related to the group velocity dispersion (GVD) and the self-phase modulation (SPM), respectively. On the other hand, in the subpicosecond or femtosecond regime, the NLS equation has been claimed to be inadequate since the optical pulse becomes shorter [5,6]. Thus, it becomes absolutely necessary to include the third-order dispersion (TOD), the self-steepening (SS), and the stimulated Raman scattering (SRS) as considered in [7]

$$E_z = i(\alpha_1 E_{tt} + \alpha_2 |E|^2 E) + \varepsilon[\alpha_3 E_{ttt} + \alpha_4 (|E|^2 E)_t + \alpha_5 E(|E|^2)_t]. \tag{2}$$

[a] e-mail: Aly742001@yahoo.com (corresponding author)

Equation (2) is a higher-order nonlinear Schrödinger (HNLS) equation. In this equation, E is the slowly varying envelope of the electric field, the subscripts z and t are the spatial and temporal partial derivatives, and α_1, α_2, α_3, α_4, and α_5, are the parameters related to the GVD, the SPM, the TOD, the SS, and the SRS, respectively. Now, if $\varepsilon = 0$, eq. (2) reduces to the NLS equation. This higher-order equation was derived by Kodama *et al.* [8,9] and using perturbation theory they treated all higher-order terms as perturbation to the NLS soliton. The main advantage of eq. (2) is that the self-frequency shift is a potentially detrimental effect in soliton communication systems because power fluctuations at the source translate into frequency fluctuations in the fiber through the power dependence of the soliton self-frequency shift and hence into timing jitter at the receiver [10].

Our objective here is to find new exact solutions of this equation. Over the last few years, finding the appropriate solutions of nonlinear equations have been the subject of intense investigation. In this context, several methods have been proposed by researchers in the literature. We can list the projective Riccati equation method [11], the Backlund transformation, inverse scattering method [12], the Hirota bilinear forms, the pseudo spectral method, the tanh-sech method [13], the Darboux transform method [14], the Painlevé's singularity structure analysis [15], the homotopy perturbation method [16], the variational iteration method [17], the inverse scattering transform method [18], the (G'/G)-expansion method [19], the Hirota's bilinear method [20], the exp-function method [21], the $\exp(-\phi(\varepsilon))$-expansion method [22], the modified simple equation method [23], the exponential rational function method [24,25], the semi-inverse variational principle [26], the Bilinear representation [27], the generalized tanh-coth method [28], the modified extended direct algebraic method [29], the auxiliary equation method [30], and so on [31–48].

The rest of the paper is structured as follows: In sect. 2, we discuss the bifurcations of phase portraits of the model studied. In sect. 3, we find the solutions of the model using arbitrary nonlinear parameters [49] and the exponential rational function method. The graphical representations are given in sect. 4. Finally, sect. 5 concludes the work.

2 Phase portraits of the model

We consider the one-dimensional HNLS equation which reads,

$$E_z = i(\alpha_1 E_{tt} + \alpha_2 |E|^2 E) + \varepsilon[\alpha_3 E_{ttt} + \alpha_4 (|E|^2 E)_t + \alpha_5 E(|E|^2)_t]. \tag{3}$$

We assume a solution given by the following expression:

$$E(z,t) = A(\xi)e^{i\theta}, \tag{4}$$

where $\xi = \delta t + uz$ and $\theta = \beta t + rz$; $A(\xi)$ is a real amplitude function, δ, u, β and r are real parameters. Substituting eq. (4) into eq. (3) and separating real and imaginary parts, we obtain

$$Im : -(\varepsilon\alpha_4\beta + \alpha_2)A^3 + (r + \alpha_1\beta^2 + \varepsilon\alpha_3\beta^3)A - (\alpha_1\delta^2 + 3\alpha_3\varepsilon\beta\delta^2)A'' = 0, \tag{5}$$

$$Re : (u + 2\alpha_1\beta\delta + 3\alpha_3\varepsilon\beta^2\delta)A' - (3\varepsilon\alpha_4\delta + 2\varepsilon\alpha_5\delta)A^2A' - \varepsilon\alpha_3\delta^3A''' = 0. \tag{6}$$

It is possible to integrate eq. (6) because it has only first- and third-order derivatives. We then have

$$-\frac{u + 2\alpha_1\beta\delta + 3\alpha_3\varepsilon\beta^2\delta}{\varepsilon\alpha_3\delta^3}A + \frac{\alpha_4 + (2/3)\alpha_5}{\alpha_3\delta^2}A^3 + A'' = 0. \tag{7}$$

Comparing eqs. (7) and (5) the parameters β and r can be evaluated in the form

$$\beta = -\frac{3\alpha_1\alpha_4 + 2\alpha_1\alpha_5 - 3\alpha_2\alpha_3}{6\varepsilon\alpha_3(\alpha_4 + \alpha_5)}, \tag{8}$$

and

$$r = -\frac{8\beta^3\delta\varepsilon^2\alpha_3^2 + 8\beta^2\delta\varepsilon\alpha_1\alpha_3 + 2\beta\delta\alpha_1^2 + 3\beta\varepsilon u\alpha_3 + u\alpha_1}{\delta\varepsilon\alpha_3}. \tag{9}$$

Therefore, eqs. (5) and (7) have similar form and we concentrate ourselves on eq. (5) from which the first integral is obtained by multiplying it by A' and integrating the resulting equation:

$$A'^2 - \frac{r + \alpha_1\beta^2 + \varepsilon\alpha_3\beta^3}{\alpha_1\delta^2 + 3\alpha_3\varepsilon\beta\delta^2}A^2 + \frac{\varepsilon\alpha_4\beta + \alpha_2}{2(\alpha_1\delta^2 + 3\alpha_3\varepsilon\beta\delta^2)}A^4 = 2C, \tag{10}$$

where C is the constant of integration. Let us mention that, eq. (10) can be also derived from the auxiliary Hamiltonian $\widetilde{H}$ and lagrangian $\widetilde{L}$ defined by

$$\widetilde{H} = \frac{1}{2}m(A)[A'^2 + U(A)] \tag{11}$$

and

$$\widetilde{L} = \frac{1}{2}m(A)[A'^2 - U(A)]. \tag{12}$$

This Hamiltonian may be viewed as the energy of a particle with an effective mass $m(A) = 1$ moving in the effective potential

$$U(A) = -\frac{r + \alpha_1\beta^2 + \varepsilon\alpha_3\beta^3}{\alpha_1\delta^2 + 3\alpha_3\varepsilon\beta\delta^2}A^2 + \frac{\varepsilon\alpha_4\beta + \alpha_2}{2(\alpha_1\delta^2 + 3\alpha_3\varepsilon\beta\delta^2)}A^4 - 2C. \tag{13}$$

It is obvious that eq. (5) can be transformed into the following equivalent autonomous dynamic system:

$$\begin{cases} \dfrac{\mathrm{d}A}{\mathrm{d}\xi} = A', \\ \dfrac{\mathrm{d}A'}{\mathrm{d}\xi} = \left[-\dfrac{\varepsilon\alpha_4\beta + \alpha_2}{\alpha_1\delta^2 + 3\alpha_3\varepsilon\beta\delta^2}A^2 + \dfrac{r + \alpha_1\beta^2 + \varepsilon\alpha_3\beta^3}{\alpha_1\delta^2 + 3\alpha_3\varepsilon\beta\delta^2}\right]A, \end{cases} \tag{14}$$

where solutions are the fixed points of the system. The behavior of this system may be easily studied by means of the phase plane plot which is the best tool for observing the evolution of the variable A. The number of equilibrium points, and consequently the dynamic of this system depend on the sign of the quantity

$$F_0 = \frac{r + \alpha_1\beta^2 + \varepsilon\alpha_3\beta^3}{\varepsilon\alpha_4\beta + \alpha_2}, \tag{15}$$

with $\varepsilon\alpha_4\beta + \alpha_2 \neq 0$.

For example, if $F_0 > 0$, the system (14) admits three equilibrium points: $(0, 0)$ and $(0, \pm F_{eq})$, with

$$F_{eq} = \sqrt{\frac{r + \alpha_1\beta^2 + \varepsilon\alpha_3\beta^3}{\varepsilon\alpha_4\beta + \alpha_2}}. \tag{16}$$

However, when $F_0 < 0$, the system admits only the equilibrium point $(0, 0)$. By the qualitative analysis, we obtain the different topological phase portraits shown in fig. 1 and the corresponding effective potentials in fig. 2. We observe that by changing the values of the constants α_i $(i = 1, 2, \ldots, 5)$, the behavior of the system studied change and consequently, new solutions are obtained.

3 Exact solutions of eq. (3)

3.1 Cnoidal and hyperbolic wave solutions

In this section, we shall discuss the construction of some of the physically interesting periodic solutions. These solutions will depend of the value of the constant C.

Case 1.

We set $C = -\frac{(r+\alpha_1\beta^2+\varepsilon\alpha_3\beta^3)^2 m^2}{(\alpha_1\delta^2+3\alpha_3\varepsilon\beta\delta^2)(\varepsilon\alpha_4\beta+\alpha_2)(1+m^2)^2}$ and we get the solution of eq. (10) as

$$A(\xi) = \sqrt{\frac{2(r + \alpha_1\beta^2 + \varepsilon\alpha_3\beta^3)m^2}{(\varepsilon\alpha_4\beta + \alpha_2)(1 + m^2)}}\,\mathrm{sn}\left[\sqrt{-\frac{r + \alpha_1\beta^2 + \varepsilon\alpha_3\beta^3}{(\alpha_1\delta^2 + 3\alpha_3\varepsilon\beta\delta^2)(1 + m^2)}}\xi, m\right] \tag{17}$$

and the solution of (3) is

$$E(z,t) = \sqrt{\frac{2(r + \alpha_1\beta^2 + \varepsilon\alpha_3\beta^3)m^2}{(\varepsilon\alpha_4\beta + \alpha_2)(1 + m^2)}}\,\mathrm{sn}\left[\sqrt{-\frac{r + \alpha_1\beta^2 + \varepsilon\alpha_3\beta^3}{(\alpha_1\delta^2 + 3\alpha_3\varepsilon\beta\delta^2)(1 + m^2)}}(\delta t + uz), m\right]e^{i(\beta t + rz)}. \tag{18}$$

Now, if $m \to 1$, $\mathrm{sn}(x, 1) = \tanh(x)$ and the previous solution takes the following form:

$$E(z,t) = \sqrt{\frac{r + \alpha_1\beta^2 + \varepsilon\alpha_3\beta^3}{2(\varepsilon\alpha_4\beta + \alpha_2)}}\tanh\left[\sqrt{-\frac{r + \alpha_1\beta^2 + \varepsilon\alpha_3\beta^3}{2(\alpha_1\delta^2 + 3\alpha_3\varepsilon\beta\delta^2)}}(\delta t + uz)\right]e^{i(\beta t + rz)}. \tag{19}$$

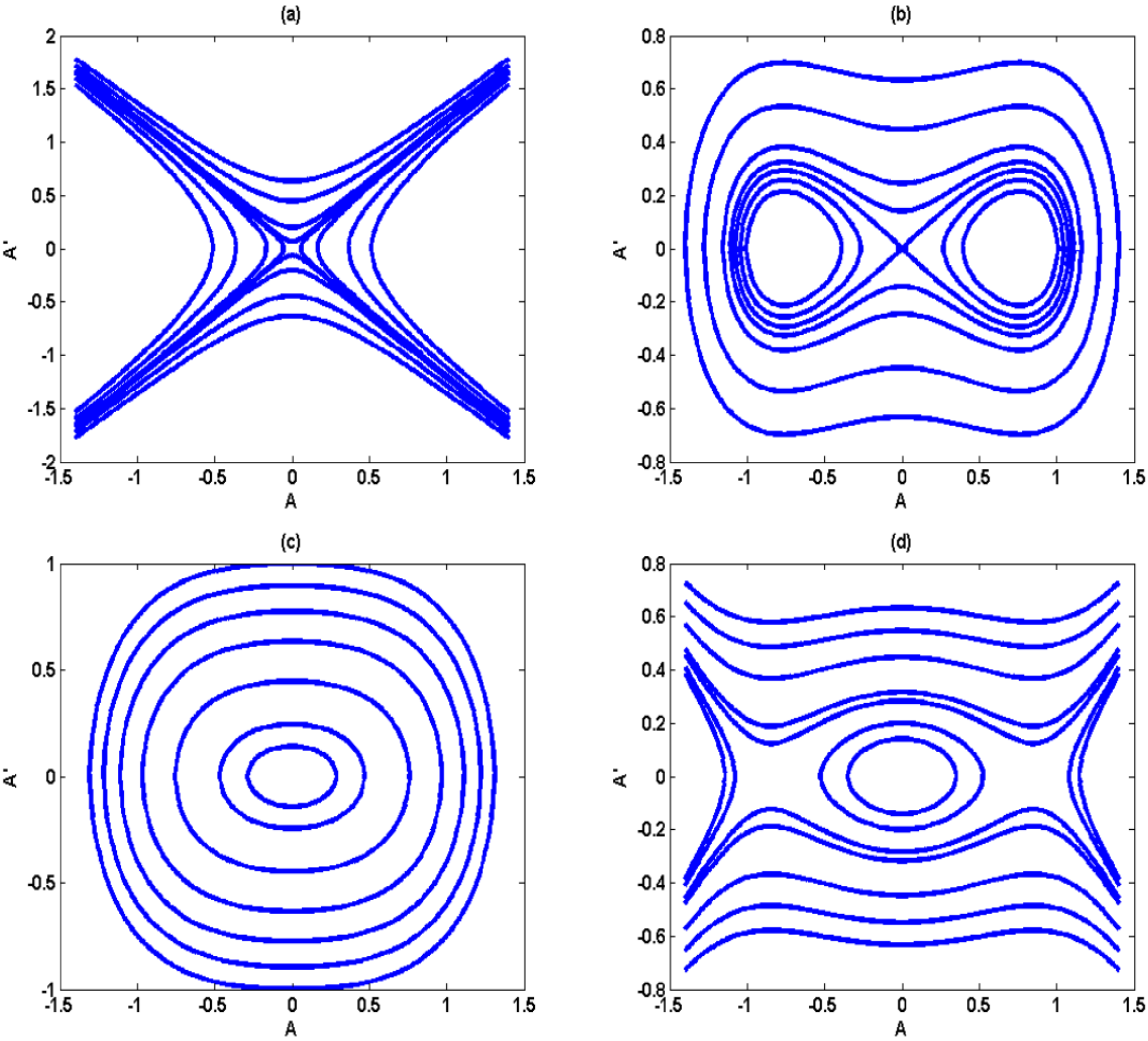

Fig. 1. Different phase portraits of the HNLS equation (2). Panel (a) is obtained for $\alpha_1 = 1.0$, $\alpha_2 = -2.0$, $\alpha_3 = 3.0$, $\alpha_4 = 1.0$, $\alpha_5 = 0.6$, $\varepsilon = 0.5$, $\delta = 2.0$ and $u = 3.0$. Panel (b) is obtained for $\alpha_1 = 1.0$, $\alpha_2 = -0.5$, $\alpha_3 = 2.0$, $\alpha_4 = 0.1$, $\alpha_5 = 6.0$, $\varepsilon = 0.5$, $\delta = 2.0$ and $u = 3.0$. Panel (c) is obtained for $\alpha_1 = 1.0$, $\alpha_2 = 2.0$, $\alpha_3 = -3.0$, $\alpha_4 = -1.0$, $\alpha_5 = -6.0$, $\varepsilon = 0.5$, $\delta = 2.0$ and $u = 3.0$. Panel (d) is obtained for $\alpha_1 = 1.0$, $\alpha_2 = 2.0$, $\alpha_3 = -3.0$, $\alpha_4 = -1.0$, $\alpha_5 = 6.0$, $\varepsilon = 0.5$, $\delta = 2.0$ and $u = 3.0$.

Case 2.

We set $C = -\frac{(r+\alpha_1\beta^2+\varepsilon\alpha_3\beta^3)^2(1-m^2)}{(\alpha_1\delta^2+3\alpha_3\varepsilon\beta\delta^2)(\varepsilon\alpha_4\beta+\alpha_2)(2-m^2)^2}$ and we get the solution of eq. (10) as

$$A(\xi) = \sqrt{\frac{2(r+\alpha_1\beta^2+\varepsilon\alpha_3\beta^3)}{(\varepsilon\alpha_4\beta+\alpha_2)(2-m^2)}}\,\mathrm{dn}\left[\sqrt{\frac{r+\alpha_1\beta^2+\varepsilon\alpha_3\beta^3}{(\alpha_1\delta^2+3\alpha_3\varepsilon\beta\delta^2)(2-m^2)}}\xi, m\right], \tag{20}$$

and the solution of (3) is

$$E(z,t) = \sqrt{\frac{2(r+\alpha_1\beta^2+\varepsilon\alpha_3\beta^3)}{(\varepsilon\alpha_4\beta+\alpha_2)(2-m^2)}}\,\mathrm{dn}\left[\sqrt{\frac{r+\alpha_1\beta^2+\varepsilon\alpha_3\beta^3}{(\alpha_1\delta^2+3\alpha_3\varepsilon\beta\delta^2)(2-m^2)}}(\delta t+uz), m\right]e^{i(\beta t+rz)}. \tag{21}$$

Now, if $m \to 1$, $\mathrm{dn}(x,1) = \mathrm{sech}(x)$ and the previous solution takes the following form:

$$E(z,t) = \sqrt{\frac{2(r+\alpha_1\beta^2+\varepsilon\alpha_3\beta^3)}{\varepsilon\alpha_4\beta+\alpha_2}}\,\mathrm{sech}\left[\sqrt{\frac{r+\alpha_1\beta^2+\varepsilon\alpha_3\beta^3}{\alpha_1\delta^2+3\alpha_3\varepsilon\beta\delta^2}}(\delta t+uz)\right]e^{i(\beta t+rz)}. \tag{22}$$

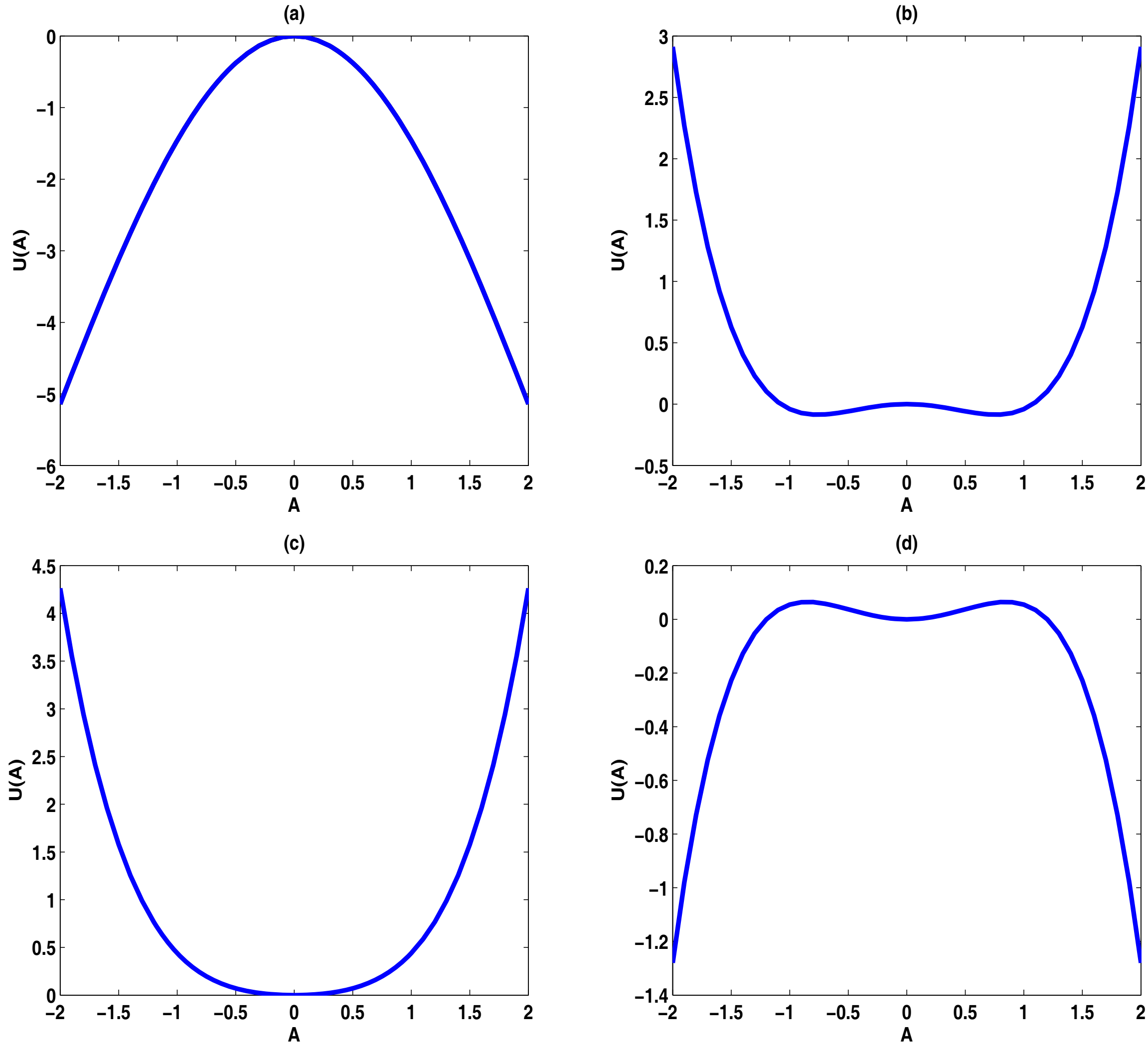

Fig. 2. Effective potential U(A) of the HNLS equation (2). These figures are obtained with the same parameters as in fig. 1. Panel (a) corresponds to phase portrait fig. 1(a); Panel (b) corresponds to phase portrait fig. 1(b); Panel (c) corresponds to phase portrait fig. 1(c); Panel (d) corresponds to phase portrait fig. 1(d).

Case 3.

We set $C = -\frac{(r+\alpha_1\beta^2+\varepsilon\alpha_3\beta^3)^2(m^2-1)m^2}{(\alpha_1\delta^2+3\alpha_3\varepsilon\beta\delta^2)(\varepsilon\alpha_4\beta+\alpha_2)(2m^2-1)^2}$ and we get the solution of eq. (10) as

$$A(\xi) = \sqrt{\frac{2m^2(r+\alpha_1\beta^2+\varepsilon\alpha_3\beta^3)}{(\varepsilon\alpha_4\beta+\alpha_2)(2m^2-1)}}\,\mathrm{cn}\left[\sqrt{\frac{r+\alpha_1\beta^2+\varepsilon\alpha_3\beta^3}{(\alpha_1\delta^2+3\alpha_3\varepsilon\beta\delta^2)(2m^2-1)}}\xi, m\right], \tag{23}$$

and the solution of (3) is

$$E(z,t) = \sqrt{\frac{2m^2(r+\alpha_1\beta^2+\varepsilon\alpha_3\beta^3)}{(\varepsilon\alpha_4\beta+\alpha_2)(2m^2-1)}}\,\mathrm{cn}\left[\sqrt{\frac{r+\alpha_1\beta^2+\varepsilon\alpha_3\beta^3}{(\alpha_1\delta^2+3\alpha_3\varepsilon\beta\delta^2)(2m^2-1)}}(\delta t+uz), m\right] e^{i(\beta t+rz)}. \tag{24}$$

Now, if $m \to 1$, $\mathrm{cn}(x,1) = \mathrm{sech}(x)$ and the previous solution takes the following form:

$$E(z,t) = \sqrt{\frac{2(r+\alpha_1\beta^2+\varepsilon\alpha_3\beta^3)}{\varepsilon\alpha_4\beta+\alpha_2}}\,\mathrm{sech}\left[\sqrt{\frac{r+\alpha_1\beta^2+\varepsilon\alpha_3\beta^3}{\alpha_1\delta^2+3\alpha_3\varepsilon\beta\delta^2}}(\delta t+uz)\right] e^{i(\beta t+rz)}. \tag{25}$$

3.2 The exponential rational function method

In this subsection, we first present the different steps of the exponential rational function method [25]:

1) Suppose that a nonlinear partial differential equation is given by

$$Q(v, v_x, v_{xx}, v_t, v_{tt}, v_{xt}, vv_x \dots) = 0. \tag{26}$$

2) To solve this equation, we reduce the number of variables to only one. Thus,

$$v(x,t) = v(\xi). \tag{27}$$

And therefore, eq. (26) constructs an ordinary differential equation (ODE) of the form

$$Q(v, v', v'', vv' \dots) = 0, \tag{28}$$

where $'$ denotes the derivation with respect to ξ. If it is possible, eq. (28) can be integrated term by term one or more times.

3) According to the present method, a solution of eq. (28) is expressed as follows:

$$v(\xi) = \sum_{i=0}^{M} \frac{\beta_i}{(1+e^{\mu\xi})^i}\,, \tag{29}$$

where μ and β_i are unknown constants which will be determined. The parameter M is determined by balancing the linear terms of the highest order in the resulting equation with the highest-order nonlinear terms. Substituting eq. (29) into eq. (28), we collect all coefficients of powers of $e^{\mu\xi}$ in the resulting equation where these coefficients have to vanish. This leads to a system of algebraic equations involving the parameters μ and β_i. Solving this system with the aid of Maple, we obtain the exact solutions of eq. (26).

Now, considering eq. (10), the balancing process gives $M = 1$ and the following solution is considered:

$$A(\xi) = \beta_0 + \frac{\beta_1}{1+e^{\mu\xi}}\,. \tag{30}$$

Substituting (30) into (10) and collecting all the coefficients of $(e^{\mu\xi})^j$ $(j = 0, 1, 2, 3, 4)$ and setting them to zero, we have the following algebraic equations:

$$(e^{\mu\xi})^4: -2\,\epsilon\,\alpha_3\beta^3{\beta_0}^2 + \epsilon\,\alpha_4\beta\,{\beta_0}^4 + \alpha_2{\beta_0}^4 - 4\,C\delta^2\alpha_1 - 12\,C\delta^2\alpha_3\epsilon\,\beta - 2\,r{\beta_0}^2 - 2\,\alpha_1\beta^2{\beta_0}^2 = 0, \tag{31}$$

$$\begin{aligned}(e^{\mu\xi})^3: &-16\,C\delta^2\alpha_1 - 8\,r{\beta_0}^2 + 4\,\epsilon\,\alpha_4\beta\,{\beta_0}^3\beta_1 + 4\,\alpha_2{\beta_0}^4 + 4\,\epsilon\,\alpha_4\beta\,{\beta_0}^4 - 8\,\alpha_1\beta^2{\beta_0}^2 - 4\,r\beta_0\beta_1\\ &-48\,C\delta^2\alpha_3\epsilon\,\beta - 4\,\epsilon\,\alpha_3\beta^3\beta_0\beta_1 - 8\,\epsilon\,\alpha_3\beta^3{\beta_0}^2 - 4\,\alpha_1\beta^2\beta_0\beta_1 + 4\,\alpha_2{\beta_0}^3\beta_1 = 0,\end{aligned} \tag{32}$$

$$\begin{aligned}(e^{\mu\xi})^2: &\,6\,\alpha_2{\beta_0}^4 - 72\,C\delta^2\alpha_3\epsilon\,\beta - 12\,r\beta_0\beta_1 - 12\,r{\beta_0}^2 - 24\,C\delta^2\alpha_1 + 6\,\epsilon\,\alpha_4\beta\,{\beta_0}^4 + 2\,{\beta_1}^2\mu^2\delta^2\alpha_1\\ &-12\,\alpha_1\beta^2{\beta_0}^2 - 2\,r{\beta_1}^2 + 12\,\alpha_2{\beta_0}^3\beta_1 - 12\,\epsilon\,\alpha_3\beta^3{\beta_0}^2 - 12\,\epsilon\,\alpha_3\beta^3\beta_0\beta_1 + 6\,\alpha_2{\beta_0}^2{\beta_1}^2\\ &-2\,\alpha_1\beta^2{\beta_1}^2 + 12\,\epsilon\,\alpha_4\beta\,{\beta_0}^3\beta_1 + 6\,{\beta_1}^2\mu^2\delta^2\alpha_3\epsilon\,\beta - 2\,\epsilon\,\alpha_3\beta^3{\beta_1}^2\\ &+6\,\epsilon\,\alpha_4\beta\,{\beta_0}^2{\beta_1}^2 - 12\,\alpha_1\beta^2\beta_0\beta_1 = 0,\end{aligned} \tag{33}$$

$$\begin{aligned}(e^{\mu\xi})^1: &\,12\,\alpha_2{\beta_0}^3\beta_1 + 12\,\alpha_2{\beta_0}^2{\beta_1}^2 - 12\,\alpha_1\beta^2\beta_0\beta_1 - 8\,r{\beta_0}^2 - 4\,\epsilon\,\alpha_3\beta^3{\beta_1}^2 + 12\,\epsilon\,\alpha_4\beta\,{\beta_0}^2{\beta_1}^2\\ &+4\,\epsilon\,\alpha_4\beta\,{\beta_0}^4 - 12\,r\beta_0\beta_1 - 16\,C\delta^2\alpha_1 - 4\,r{\beta_1}^2 + 12\,\epsilon\,\alpha_4\beta\,{\beta_0}^3\beta_1 - 48\,C\delta^2\alpha_3\epsilon\,\beta\\ &+4\,\alpha_2\beta_0{\beta_1}^3 - 8\,\alpha_1\beta^2{\beta_0}^2 + 4\,\epsilon\,\alpha_4\beta\,\beta_0{\beta_1}^3 - 4\,\alpha_1\beta^2{\beta_1}^2 - 8\,\epsilon\,\alpha_3\beta^3{\beta_0}^2\\ &-12\,\epsilon\,\alpha_3\beta^3\beta_0\beta_1 + 4\,\alpha_2{\beta_0}^4 = 0,\end{aligned} \tag{34}$$

$$\begin{aligned}(e^{\mu\xi})^0: &\,\epsilon\,\alpha_4\beta\,{\beta_0}^4 - 2\,\epsilon\,\alpha_3\beta^3{\beta_0}^2 + 4\,\alpha_2{\beta_0}^3\beta_1 - 4\,\alpha_1\beta^2\beta_0\beta_1 - 2\,\epsilon\,\alpha_3\beta^3{\beta_1}^2 - 2\,\alpha_1\beta^2{\beta_1}^2\\ &-4\,r\beta_0\beta_1 - 2\,r{\beta_1}^2 + 6\,\epsilon\,\alpha_4\beta\,{\beta_0}^2{\beta_1}^2 + \alpha_2{\beta_1}^4 + 4\,\epsilon\,\alpha_4\beta\,\beta_0{\beta_1}^3 + 4\,\epsilon\,\alpha_4\beta\,{\beta_0}^3\beta_1\\ &+6\,\alpha_2{\beta_0}^2{\beta_1}^2 + \epsilon\,\alpha_4\beta\,{\beta_1}^4 - 2\,r{\beta_0}^2 - 2\,\alpha_1\beta^2{\beta_0}^2 - 4\,\epsilon\,\alpha_3\beta^3\beta_0\beta_1 - 12\,C\delta^2\alpha_3\epsilon\,\beta\\ &+4\,\alpha_2\beta_0{\beta_1}^3 + \alpha_2{\beta_0}^4 - 4\,C\delta^2\alpha_1 = 0.\end{aligned} \tag{35}$$

Solving the above algebraic eqs. (31)–(35), we have the following sets of coefficients:

Set 1:

$$\beta_0=\sqrt{\frac{r+\alpha_1\beta^2+\varepsilon\alpha_3\beta^3}{\varepsilon\alpha_4\beta+\alpha_2}}\,,\qquad \beta_1=-2\sqrt{\frac{r+\alpha_1\beta^2+\varepsilon\alpha_3\beta^3}{\varepsilon\alpha_4\beta+\alpha_2}}\,,$$
$$C=-\frac{1}{4}\frac{(r+\alpha_1\beta^2+\varepsilon\alpha_3\beta^3)^2}{\delta^2(\varepsilon\alpha_4\beta+\alpha_2)(\alpha_1+3\alpha_3\varepsilon\beta)}\,,\qquad \mu=\eta\sqrt{\frac{2(r+\alpha_1\beta^2+\varepsilon\alpha_3\beta^3)}{\delta^2(\alpha_1+3\alpha_3\varepsilon\beta)}}\,.$$

Set 2:

$$\beta_0=-\sqrt{\frac{r+\alpha_1\beta^2+\varepsilon\alpha_3\beta^3}{\varepsilon\alpha_4\beta+\alpha_2}}\,,\qquad \beta_1=2\sqrt{\frac{r+\alpha_1\beta^2+\varepsilon\alpha_3\beta^3}{\varepsilon\alpha_4\beta+\alpha_2}}\,,$$
$$C=-\frac{1}{4}\frac{(r+\alpha_1\beta^2+\varepsilon\alpha_3\beta^3)^2}{\delta^2(\varepsilon\alpha_4\beta+\alpha_2)(\alpha_1+3\alpha_3\varepsilon\beta)}\,,\qquad \mu=\eta\sqrt{\frac{2(r+\alpha_1\beta^2+\varepsilon\alpha_3\beta^3)}{\delta^2(\alpha_1+3\alpha_3\varepsilon\beta)}}\,.$$

In this subsection, the solutions of the HNLS equation depend of the constant $\frac{r+\alpha_1\beta^2+\varepsilon\alpha_3\beta^3}{\alpha_1+3\alpha_3\varepsilon\beta}$.

Case 1.

If $\frac{r+\alpha_1\beta^2+\varepsilon\alpha_3\beta^3}{\alpha_1+3\alpha_3\varepsilon\beta}>0$, we have as solutions

$$E(z,t)=\sqrt{\frac{r+\alpha_1\beta^2+\varepsilon\alpha_3\beta^3}{\varepsilon\alpha_4\beta+\alpha_2}}\left[1-\frac{2}{1+\cosh\left(\sqrt{\frac{2(r+\alpha_1\beta^2+\varepsilon\alpha_3\beta^3)}{\delta^2(\alpha_1+3\alpha_3\varepsilon\beta)}}\xi\right)+\eta\sinh\left(\sqrt{\frac{2(r+\alpha_1\beta^2+\varepsilon\alpha_3\beta^3)}{\delta^2(\alpha_1+3\alpha_3\varepsilon\beta)}}\xi\right)}\right]e^{i(\beta t+rz)},\quad(36)$$

for set 1 and

$$E(z,t)=-\sqrt{\frac{r+\alpha_1\beta^2+\varepsilon\alpha_3\beta^3}{\varepsilon\alpha_4\beta+\alpha_2}}\left[1-\frac{2}{1+\cosh\left(\sqrt{\frac{2(r+\alpha_1\beta^2+\varepsilon\alpha_3\beta^3)}{\delta^2(\alpha_1+3\alpha_3\varepsilon\beta)}}\xi\right)+\eta\sinh\left(\sqrt{\frac{2(r+\alpha_1\beta^2+\varepsilon\alpha_3\beta^3)}{\delta^2(\alpha_1+3\alpha_3\varepsilon\beta)}}\xi\right)}\right]e^{i(\beta t+rz)},\quad(37)$$

for set 2.

Case 2.

If $\frac{r+\alpha_1\beta^2+\varepsilon\alpha_3\beta^3}{\alpha_1+3\alpha_3\varepsilon\beta}<0$, we have $\mu=i\eta\sqrt{-\frac{2(r+\alpha_1\beta^2+\varepsilon\alpha_3\beta^3)}{\delta^2(\alpha_1+3\alpha_3\varepsilon\beta)}}$ with $-\frac{r+\alpha_1\beta^2+\varepsilon\alpha_3\beta^3}{\alpha_1+3\alpha_3\varepsilon\beta}>0$ and the solutions are

$$E(z,t)=\sqrt{\frac{r+\alpha_1\beta^2+\varepsilon\alpha_3\beta^3}{\varepsilon\alpha_4\beta+\alpha_2}}\left[1-\frac{2}{1+\cos\left(\sqrt{-\frac{2(r+\alpha_1\beta^2+\varepsilon\alpha_3\beta^3)}{\delta^2(\alpha_1+3\alpha_3\varepsilon\beta)}}\xi\right)+i\eta\sin\left(\sqrt{-\frac{2(r+\alpha_1\beta^2+\varepsilon\alpha_3\beta^3)}{\delta^2(\alpha_1+3\alpha_3\varepsilon\beta)}}\xi\right)}\right]e^{i(\beta t+rz)},\quad(38)$$

for set 1 and

$$E(z,t)=\sqrt{\frac{r+\alpha_1\beta^2+\varepsilon\alpha_3\beta^3}{\varepsilon\alpha_4\beta+\alpha_2}}\left[-1+\frac{2}{1+\cos\left(\sqrt{-\frac{2(r+\alpha_1\beta^2+\varepsilon\alpha_3\beta^3)}{\delta^2(\alpha_1+3\alpha_3\varepsilon\beta)}}\xi\right)+i\eta\sin\left(\sqrt{-\frac{2(r+\alpha_1\beta^2+\varepsilon\alpha_3\beta^3)}{\delta^2(\alpha_1+3\alpha_3\varepsilon\beta)}}\xi\right)}\right]e^{i(\beta t+rz)},\quad(39)$$

for set 2.

In all these solutions, $\xi=\delta t+uz$ and $\eta=\pm1$; r and β are given by eq. (8) and eq. (9), respectively; δ and u are arbitrary constants.

4 Graphical representations

The results obtained in this work are cnoidal solutions, kink solutions, pulse solutions and trigonometric solutions. These solutions can be utilized to transport information in optical fibers. We plot some solutions to have an idea on the mechanism of the original eq. (3). Specifically, we plot solutions (18), (21) and (24), this by taking suitable values of the parameters obtained. The graphical representations of these solutions are shown in figs. 3, 4, and 5.

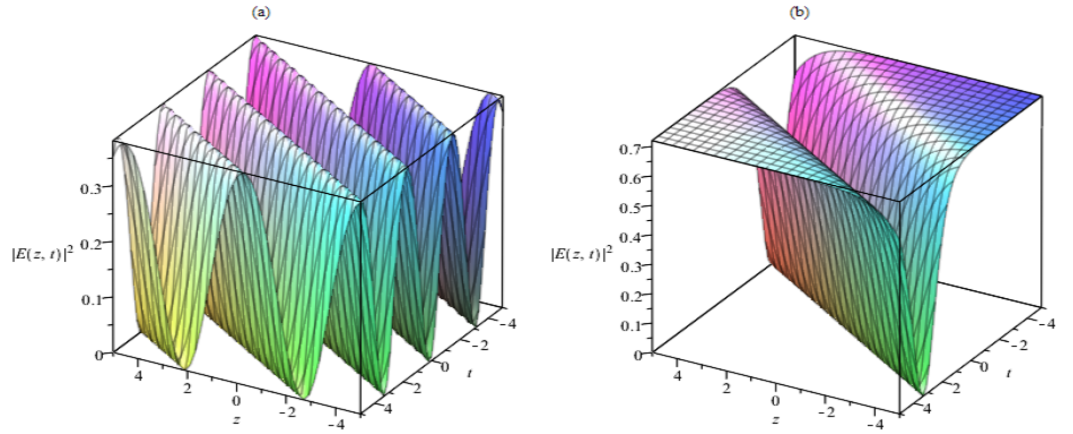

Fig. 3. Solution corresponding to eq. (18). These figures are obtained with the following parameters: $\alpha_1 = 1.0$, $\alpha_2 = 2.0$, $\alpha_3 = -3.0$, $\alpha_4 = -1.0$, $\alpha_5 = 6.0$, $\varepsilon = 0.5$, $\delta = 2.0$ and $u = 3.0$. Panel (a) is plotted for $m = 0.6$, while panel (b) is plotted for $m = 1.0$.

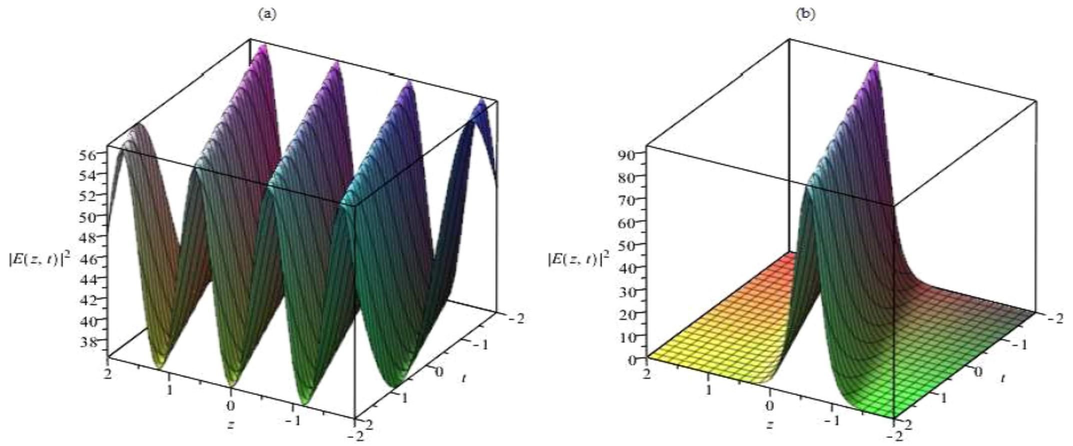

Fig. 4. Solution corresponding to eq. (21). These figures are obtained with the following parameters: $\alpha_1 = 0.1$, $\alpha_2 = 2.0$, $\alpha_3 = -3.0$, $\alpha_4 = -1.0$, $\alpha_5 = 0.1$, $\varepsilon = 0.5$, $\delta = 10.0$ and $u = 3.0$. Panel (a) is plotted for $m = 0.6$, while panel (b) is plotted for $m = 1.0$.

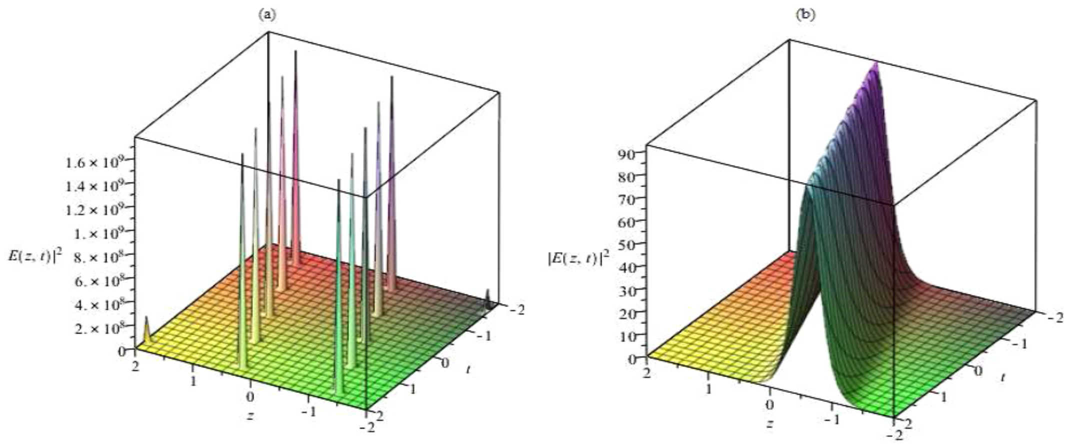

Fig. 5. Solution corresponding to eq. (24). These figures are obtained with the same parameters as in fig. 4. Panel (a) is plotted for $m = 0.6$, while panel (b) is plotted for $m = 1.0$.

5 Conclusion

By using the arbitrary nonlinear parameters and the exponential rational function method, we find in this work many new exact solutions of the higher-order nonlinear Schrödinger equation. The solutions obtained by the current methods are cnoidal solutions, kink solutions, pulse solutions and trigonometric solutions. By adjusting, for example, the modulus of some solutions obtained ($m = 0.6, 1$), the shape of solutions can be well controlled. Optical soliton solutions obtained here can be used to transport information in telecommunication domain and in many other domains like nonlinear electrical transmission lines or nonlinear chains of atoms to list a few. It also comes from this work that the behavior of this HNLS equation may be easily studied by means of the phase plane plot which is the best tool to predict some solutions. The behavior of these phase portraits are confirmed by the corresponding effective potentials. It is also important to mention that the solutions found in this paper are new solutions of the model not yet reported in the literature.

References

1. J.S. Russell, *Report of the fourteenth meeting of the British Association for the Advancement of Science, York, September 1844* (London, 1845) pp. 311–390, Plates XLVII-LVII.
2. A. Hasegawa, F. Tappert, Appl. Phys. Lett. **23**, 142 (1973).
3. L.F. Mollenauer, R.H. Stolen, J.P. Gordon, Phys. Rev. Lett. **45**, 1095 (1980).
4. G.B. Whithman, *Linear and Nonlinear Waves* (Wiley, New York, 1974) chapt. 17.
5. G.P. Agrawal, *Nonlinear Fiber Optics* (Academic Press, New York, 2001).
6. C. Zhao, Y.T. Gao, Z.Z. Lan, J.W. Yang, C.Q. Su, Phys. Lett. B **30**, 1650312 (2016).
7. K. Porsezian, K. Nakkeeran, Phys. Rev. Lett. **76**, 3955 (1996).
8. Y. Kodama, A. Hasegawa, IEEE J. Quantum Electron. **23**, 510 (1987).
9. Y. Kodama, J. Stat. Phys. **39**, 597 (1985).
10. D. Wood, IEEE J. Lightwave Technol. **8**, 1097 (1990).
11. R. Conte, M. Musette, J. Phys. A **25**, 5609 (1992).
12. M.J. Ablowitz, B.M. Herbst, C. Schober, J. Comput. Phys. **126**, 299 (1996).
13. W. Malfliet, W. Hereman, Phys. Scr. **54**, 563 (1996).
14. Z.S. Yersultanova, M. Zhassybayeva, K. Yesmakhanova, G. Nugmanova, R. Myrzakulov, Int. J. Geom. Methods Mod. Phys. **13**, 1550134 (2016).
15. R.S. Banerjee, Phys. Scr. **57**, 598 (1998).
16. D. Mehdi, S. Fatemeh, Phys. Scr. **75**, 778 (2007).
17. J.H. He, Phys. Scr. **76**, 680 (2007).
18. V.O. Vakhnenko, E.J. Parkes, A.J. Morrison, Chaos, Solitons Fractals **17**, 683 (2003).
19. E. Tala-Tebue, D.C. Tsobgni-Fozap, A. Kenfack-Jiotsa, T.C. Kofane, Eur. Phys. J. Plus **129**, 136 (2014).
20. R. Hirota, Phys. Rev. Lett. **27**, 1192 (1971).
21. M.B. Laila Assas, J. Comput. Appl. Math. **233**, 97 (2009).
22. K. Hosseini, A. Bekir, R. Ansari, Opt. Quantum Electron. **49**, 131 (2017).
23. A.J.M. Jawad, M.D. Petkovic, A. Biswas, Appl. Math. Comput. **217**, 869 (2010).
24. E. Tala-Tebue, Z.I. Djoufack, E. Fendzi-Donfack, A. Kenfack-Jiotsa, T.C. Kofane, Optik **127**, 11124 (2016).
25. E. Tala-Tebue, Z.I. Djoufack, D.C. Tsobgni-Fozap, A. Kenfack-Jiotsa, F. Kapche-Tagne, T.C. Kofané, Chin. J. Phys. **55**, 939 (2017).
26. A. Biswas, M. Zaka Ullah, M. Asma, Q. Zhou, P. Seithuti, M. Belic, Optik **139**, 16 (2017).
27. F. Lian-Li, T. Shou-Fu, H. Yan, L. Wang, Z. Tian-Tian, Eur. Phys. J. Plus **131**, 241 (2016).
28. J. Manafian, M. Lakestani, Indian J. Phys. **91**, 243 (2017).
29. Lu Dianchen, Aly R. Seadawy, M. Arshad, Opt. Quantum Electron. **50**, 23 (2018).
30. U.T. Kalim, Aly R. Seadawy, Optik **154**, 785 (2018).
31. Aly Seadawy, Jalil Manafian, Results Phys. **8**, 1158 (2018).
32. Mehdi Dehghan, Jalil Manafian, Abbas Saadatmandi, Numer. Methods Partial Differ. Equ. **26**, 448 (2010).
33. Jalil Manafian, Optik **127**, 4222 (2016).
34. Mohammadreza Foroutan, Isa Zamanpour, Jalil Manafian, Eur. Phys. J. Plus **132**, 421 (2017).
35. Jalil Manafian, Eur. Phys. J. Plus **130**, 255 (2015).
36. Jalil Manafiana, Mehdi Fazli Aghdaeib, Morteza Khalilianc, Ramin Sarbaz Jeddi, Optik **135**, 395 (2017).
37. Cevat Teymuri Sindi, Jalil Manafian, Eur. Phys. J. Plus **132**, 67 (2017).
38. Jalil Manafian, Jalal Jalali, Arash Ranjbaran, Opt. Quantum Electron. **49**, 406 (2017).
39. Jalil Manafian, Mehrdad Lakestani, Optik **127**, 5543 (2016).
40. Asghar Ali, Aly Seadawy, Dianchen Lu, Optik **145**, 79 (2017).
41. Aly Seadawy, Eur. Phys. J. Plus **132**, 518 (2017).
42. Aly R. Seadawy, Pramana J. Phys. **89**, 49 (2017).
43. Aly Seadawy, J. Electromagn. Waves Appl. **31**, 1353 (2017).

44. Aly Seadawy, Optik **139**, 31 (2017).
45. Aly R. Seadawy, Eur. Phys. J. Plus **132**, 29 (2017).
46. A.H. Khater, D.K. Callebaut, W. Malfliet, A.R. Seadawy, Phys. Scr. **64**, 533 (2001).
47. A.H. Khater, D.K. Callebaut, A.R. Seadawy, Phys. Scr. **67**, 340 (2003).
48. Aly R. Seadawy, Dipankar Kumar, Anuz Kumar Chakrabarty, Eur. Phys. J. Plus **133**, 182 (2018).
49. H. Triki, A. Biswas, D. Milović, M. Belić, Acta Phys. Pol. A **130**, 718 (2016).